This is a preproof accepted article for *Mineralogical Magazine*
This version may be subject to change during the production process
DOI: 10.1180/mgm.2025.10149

Polythermal studies of weeksite, a microporous uranyl silicate, and its synthetic analogues

Evgeny V. Nazarchuk[a], Oleg I. Siidra[a,b*], Yana G. Tagirova[a], Dmitri O. Charkin[c], Jakub Plášil[d], Anatoly V. Kasatkin[e], Stepan N. Kalmykov[c], Dmitri N. Dmitriev[c]

[a] Department of Crystallography, Saint-Petersburg State University, University emb. 7/9, St. Petersburg 199034, Russia

[b] Kola Science Center, Russian Academy of Sciences, Apatity, Murmansk Region, 184200, Russia

[c] Department of Chemistry, Moscow State University, Vorobievy Gory 1, bd. 3, Moscow 119991, Russia

[d] Institute of Physics of the CAS, v.v.i., Na Slovance 2, CZ-182 00, Praha 8, Czech Republic

[e] Fersman Mineralogical Museum of the Russian Academy of Sciences, Leninskiy pr. 18, 2, 119071, Moscow, Russia

*o.siidra@spbu.ru
Received; accepted

Abstract

We investigated crystal structures and the mechanism of thermal expansion of weeksite and its synthetic analogs (K-, Rb-, Cs-) using a combination of geometrical-topological analysis and empirical methods (powder X-ray diffraction, infrared spectroscopy, scanning electron microscopy, single-crystal and powder X-ray variable-temperature diffraction). The weeksite sample studied herein was collected at the Anderson mine, Yavapai County, Arizona, U.S.A. Its synthetic analogs were prepared using high-temperature approaches in sealed silica tubes. Natural weeksite is stable until 860 ± 10 ºC; it dehydrates between 100 - 200 ºC. Its synthetic analogs with Rb and Cs are stable at least until 1000 ºC. Their thermal expansion is strongly anisotropic due to shear deformations of the crystal structure. The framework in the structure of weeksite can be regarded as a sequence of uranyl silicate layers linked by SiO_4 tetrahedra. With increasing temperature, the angles at the Si-O-Si "hinges" change essentially, which causes the shear deformations. The differences in the thermal behavior, including expansion anisotropy, are likely due to the nature (size) of the alkali cations occupying the cavities in the framework. The partial or complete replacement of Rb^+ by Cs^+ illustrates the zeolite-like nature of the uranyl silicate framework in weeksite. Therefore, its structure can be considered a possible candidate for the selective

immobilization of $^{137}Cs^{+}$ upon storing nuclear waste with little interference from the more abundant Na^{+} and K^{+}.

Keywords: weeksite, uranyl oxysalts, silicates, microporous structures, inorganic synthesis, ion-exchange

1. Introduction

Silicates of hexavalent uranium are readily formed in the oxidation areas of primary uranium deposits and during the processing and storage of spent nuclear fuel and radioactive waste. Experiments modeling the latter processes have demonstrated (Wronkiewicz *et al*., 1996) that uranyl silicates, *e.g.* uranophane $Ca[(UO_2)_2(SiO_3OH)_2](H_2O)_5$, boltwoodite, $(K,Na)[(UO_2)(SiO_3OH)](H_2O)_{1.5}$, and weeksite, $K_2[(UO_2)_2(Si_5O_{13})](H_2O)_4$ dominate upon crystallization of modified underground waters (Finch *et al*., 1999) or upon oxidation of actinide- bearing borosilicate waste glass (Burns *et al*., 2000), as well as among products of interaction between simulated nuclear wastes and crystalline silicate rocks (Oji *et al*., 2006). Uranyl silicates are known to incorporate radionuclides into their crystal structures (Burns *et al*., 1997) and retard their migration from the storage site (Chen *et al*., 2000). Therefore, studies of uranyl silicates, elucidating the structural origins of nuclide incorporation and their physical properties, are of essential importance. Understanding their structural peculiarities and trends is believed to provide clues to the long-term effectiveness of the geological storage of radioactive wastes (Jackson and Burns, 2000). While not numerous, uranyl silicates exhibit wide structural diversity due to the ability of the uranyl and silicate tetrahedra to condense by sharing edges and vertices, respectively (Nazarchuk *et al*., 2023a). This commonly leads to the formation of microporous frameworks, as well as nanotubular architectures (Nazarchuk *et al*., 2023b).

Weeksite was first discovered by W.F. Outerbridge at the Thomas Range deposit, Juab County, Utah, in 1960 (Outerbridge *et al*., 1960). The crystal structure of weeksite had been refined in various space groups and unit cells. It was initially reported as orthorhombic and several space groups were suggested: *Cmmb* (Jackson and Burns, 2000), *C*2*mm* or *C*222 (Babo and Albrecht-Schmitt, 2013), and *Cmmm* (Plesko *et al*., 1992; Baturin and Sidorenko, 1985). Finally, Fejfarová *et al*. (2012) reported a solution in monoclinic symmetry, *C*2/*m*, a = 14.1957(4), b = 14.2291(5), c = 9.6305(3) Å, and β = 111.578(3)°, which involves twinning of the monoclinic structure by reticular merohedry and simulates orthorhombic lattice. We notice that the model twinning reported directly in the text of the paper by Fejfarová *et al*. (2012) is incorrect. The correct model (reticular twin, diffraction type II; Petříček *et al*. 2016)

https://doi.org/10.1180/mgm.2025.10149 Published online by Cambridge University Press

involves a two-fold axis operation (or mirror, as an alternative co-set) in (101), which leads to an orthorhombic lattice of four-times larger volume of the unit-cell (*a*~14.22 Å, *b*~14.26 Å, *c*~35.95 Å, β = 90.02°, *V* = 4*1822 Å^3). Examples of how the different twin ratios affect the single-crystal X-ray diffraction pattern are given in Supplementary material ((Figure S1)). Diffraction patterns of the twin crystal were calculated using Jana2020 program (Petříček *et al.*, 2023).

The crystal structure of weeksite can be described as a microporous zeolite-like framework containing channels with an effective size of up to 5.00×0.80 and 6.21×6.21 Å^2 in *ab* plane and 6.98×0.98 Å^2 in *bc* plane. Framework is relatively stable against variations of the alkali cation. Based on the chemical analysis of weeksite, Outerbridge *et al*. (1960) suggested that the alkali sites in the channels are partially occupied by Na, Ca, and Ba. Yeremenko *et al*. (1977) reported the presence of Na, Mg, Ba, and Sr in the samples from Afghanistan, Jackson and Burns (2000) found Ba and Ca, while Fejfarová *et al*. (2012) found Ba, Na and Ca. This indicates that the interiors of the uranyl-silicate framework cannot only accommodate essential amounts of water and alkali cations and are wide enough to provide their easy migration. One can suggest, therefore, that this structure would also permit an easy exchange of one alkali cation by another, which is of particular importance considering the essential presence of high-yield radioactive cesium isotopes, particularly ^{134}Cs, ^{137}Cs and long-lived ^{135}Cs (Cook *et al*. 1964; Zhu *et al*. 2021) of which two former pose immediate while the latter, delayed threat. A radioactive isotope of rubidium, ^{88}Rb, is also abundantly formed upon fission (Yanzhong and Jianzhu, 2002) but poses no actual threat as being very short-lived with $T_{1/2}$ = 17 min; of more essential concern is the very long-living though less active ^{87}Rb. As noted above, the uranyl silicates formed *in situ* are likely to affect the release of radioactive cesium isotopes; therefore, studies of weeksite's ability to incorporate alkali cations, particularly Cs^+, are important.

Depending on the conditions, uranyl silicates can reversibly hydrate and dehydrate (Chernikov *et al*., 1977, 1978). For minerals, humidity and temperature can affect their optical properties (Baturin and Sidorenko, 1985). According to DTA results, weeksite exhibits several endothermal effects accompanied by mass loss of up to 5.5 wt% (Frost *et al*., 2006). The first and most pronounced effect takes place at 100 °C (Baturin and Sidorenko, 1985; Fejfarová *et al*., 2012), or at 130 °C (Chernorukov *et al*., 2007), while two weaker ones, at 350 and 700 °C (Fejfarová *et al*., 2012).

In the current paper, we report the synthesis, polythermal single-crystal and powder X-ray studies of weeksite and its K-, Rb-, and Cs-analogs. Ion-exchange properties are

https://doi.org/10.1180/mgm.2025.10149 Published online by Cambridge University Press

reported for the Rb-analog to show the zeolitic nature of the weeksite uranyl silicate framework.

2. Experimental

2.1 Samples and occurrence

The crystals of weeksite (Figure 1a, b) were collected at the Anderson mine, Yavapai County, Arizona, U.S.A. In the selected samples, weeksite associates mainly with carnotite, quartz, gypsum and celestine.

2.2. Synthesis

The crystals of K-, Rb-, and Cs-analogs (Figure 1c-h) were produced in a high-temperature experiment, using methods similar to those described in our previous works (Nazarchuk *et al*., 2023a,b). Mixtures of U_3O_8 (obtained by thermal decomposition of uranyl acetate at 750 °C), SiO_2, Bi_2O_3, BiF_3, and *M*Cl (preheated at 150 °C for 2-3 hrs; *M* = K, Rb, Cs) in a 2:1:1:20 molar ratio were ground, loaded in thick-walled (1.5 mm) 150-mm silica tube, evacuated, sealed, and heated to 875 °C in 24 hrs., annealed for 60 hrs., and cooled to 650 °C in 60 hrs. To prevent pressure buildup due to the expected formation of volatile products, the tubes were positioned in a vertical furnace so that their upper (cold) ends protruded slightly out. The tube walls were essentially attacked by the reaction mixtures, yet the tubes did not lose integrity, and no sublimates and/or water drops were found in the cold ends. Upon opening, solidified melts were found containing dark particles and solid metal drops; numerous druses of yellow needle-like crystals were found on the tube walls just above the surface of the charge. Subsequent studies have established the formation of synthetic weeksite analogs with all three alkali cations; these will be designated as *M*-analogs of natural weeksite.

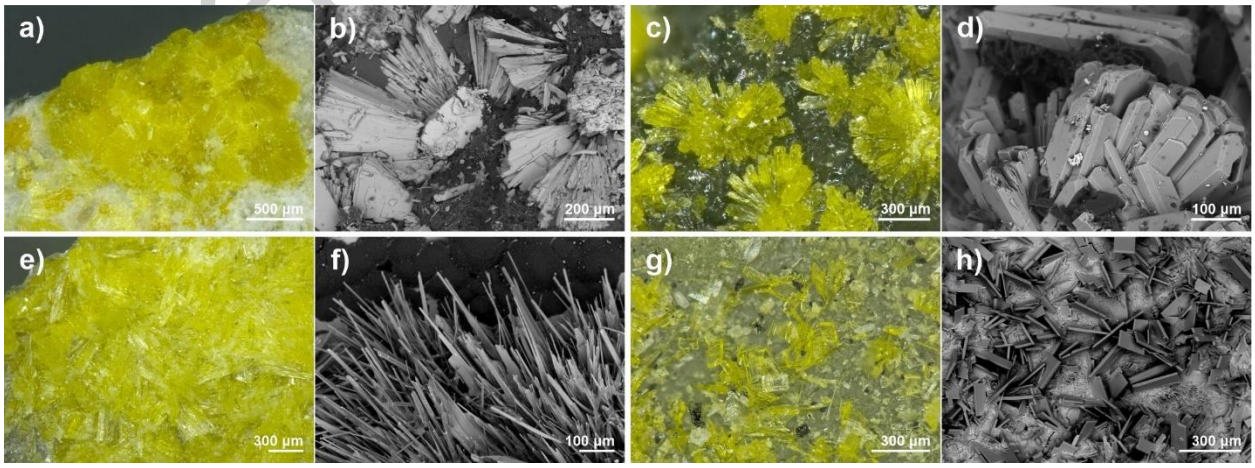

Figure 1. The crystals and SEM images of weeksite (a, b), K- (c, d), Rb- (e, f) and Cs-analogs (g, h).

https://doi.org/10.1180/mgm.2025.10149 Published online by Cambridge University Press

Initially, we used Bi_2O_3 and BiF_3 instead of PbO and HF to check which reactive fluorides, besides PbF_2, could be employed to activate uranium and silicon oxides towards reaction. At the synthesis temperatures, Bi_2O_3 is also reactive towards both silicon and uranium oxides. Hence the formation of some new multinary silicates could be expected. Yet, just like in the previous cases, only alkali uranyl silicates were produced, which are probably easiest to form due to the large excess of alkali compounds in the reaction mixtures.

2.2 Single-crystal X-ray studies

Single-crystal X-ray data of weeksite and K-, Rb-, and Cs-analogs (Table 1) were collected using a Rigaku XtaLAB Synergy-S diffractometer equipped with a PhotonJet-S detector operating with Mo*K*α radiation at 50 kV and 1 mA. Corresponding crystals were chosen for which more than a hemisphere of data was collected with a frame width of 0.5° in ω, and 5 s spent counting for each frame. The data were integrated and corrected for absorption, applying a multi-scan type (ABSCOR3) model using the Rigaku Oxford Diffraction program CrysAlis Pro.

A polythermal single-crystal experiment was conducted only for the Rb-analog, as the crystals of the K and Cs compounds were essentially smaller and would require too much time for the corresponding full-scale studies. The Rb-analog crystal was used in the temperature range of 25 – 625 ºC using a «Hot Air Gas Blowers» heating system. The starting atomic coordinates of uranium and silicon atoms were taken from Fejfarová *et al.* (2012). The structures were successfully refined using the SHELX software package (Sheldrick, 2015). Atom coordinates, thermal displacement parameters, bond lengths and calculated bond valence sums are provided in Tables S1-S11 in the supplementary materials; crystallographic data and refinement parameters are summarized in Table 1.

The effect of thermal motion on the bond-length values from single-crystal X-ray diffraction experiments is well-known (Downs, 2000). Corrections for all bonds in the studied compounds were calculated by using a formula for the rigid-body motion.

Interestingly, none of the studied crystals were twinned by above-mentioned reticular merohedry; the refined twin-fraction volumes were unsignificantly low, respectively.

https://doi.org/10.1180/mgm.2025.10149 Published online by Cambridge University Press

Table 1. Crystallographic data and refinement parameters for weeksite and its synthetic analogues.

	Mineral	K-analog	Rb-analog	Cs- analog
Temperature (K)	293(2)			
Radiation	Mo*Kα*, 0.71073			
Crystal system	monoclinic			
Space group	*C2/m*			
a (Å)	14.2183(8)	14.2156(6)	14.2907(9)	14.3448(5)
b (Å)	14.1794(6)	14.1810(4)	14.1893(6)	14.3260(7)
c (Å)	9.6229(6)	9.6212(4)	9.6137(6)	9.6209(7)
β (°)	111.445(7)	111.449(5)	111.343(7)	111.517(4)
Volume (Å^3)	1805.73(19)	1805.22(13)	1815.7(2)	1839.34(18)
D_{calc} (g/cm^3)	3.710	3.712	3.934	4.223
μ (mm^{-1})	18.804	18.809	23.558	21.898
Crystal size (mm)	0.03 × 0.12 × 0.08	0.05 × 0.16 × 0.07	0.06 × 0.12 × 0.04	0.10 × 0.12 × 0.03
θ range (°)	3.488-27.998	3.489-27.999	3.481-29.597	3.476-27.994
h, *k*, *l* ranges	–16 →18, –18 →15, –12 →9	–18 →18, –18 →18, –12 →12	–13 →19, –19 →17, –12 →11	–18 →18, –16 →18, –12 →12
Total reflections collected	2154	2262	2251	2300
Number of observed reflections	1712	1987	1797	2044
Number of least-square parameters	156	159	146	144
Unique reflections (R_{int})	0.0300	0.0392	0.0395	0.0421
Weighting scheme a, b	0.0217, 12.6292	0.0440, 4.7923	0.0375, 0.1566	0.048, 76.8738
$R_1[F > 4\sigma F]$, $wR_1[F > 4\sigma F]$	0.0271, 0.0595	0.0304, 0.0779	0.0343, 0.0811	0.0376, 0.1001
R_{all}, wR_{all}	0.0380, 0.0631	0.0345, 0.0795	0.0467, 0.0850	0.0424, 0.1023
Goodness-of-fit	1.045	1.067	1.094	1.096

2.4 Chemical composition

Selected weeksite and K-, Rb-, Cs-analog crystals were embedded into epoxy resin, polished and coated with carbon film. The chemical analyses of weeksite and its synthetic analogs were carried out with a Hitachi FlexSEM 1000 scanning electron microscope equipped with EDS Xplore Contact 30 detector and Oxford AZtecLive STD system of analysis. Analytical conditions were an accelerating voltage of 15 kV, a beam current of 5 nA and a beam size of 2 μm. The following analytical standards and X-ray lines were used: albite (Na*Kα*), KBr (K*K*α), $Rb_2Nb_4O_{11}$ (Rb*L*α), $CsDyP_4O_{12}$ (Cs*L*α), wollastonite (Ca*K*α), $BaSO_4$ (Ba*L*α), SiO_2 (Si*K*α), UO_2 (U*M*α). The contents of other elements with atomic numbers higher than that of beryllium were below detection limits. Water content was calculated based on 1) the deficiency of the total for weeksite and 2) structural data for its synthetic analogs. The analytical data are listed in Table 2.

https://doi.org/10.1180/mgm.2025.10149 Published online by Cambridge University Press

Table 2. Chemical composition (in wt%) of weeksite and its synthetic analogs (mean of 5 analyses for each)

	Weeksite			K-analog of weeksite			Rb-analog of weeksite			Cs-analog of weeksite		
	Mean	Range	SD	Mean	Range	SD	Mean	Range	SD	Mean	Range	SD
Na_2O	0.92	0.75–1.07	0.12									
K_2O	5.75	5.40–6.10	0.28	9.65	9.35–9.78	0.16						
Rb_2O							17.53	17.25–17.80	0.27			
Cs_2O										23.53	23.20–24.18	0.38
CaO	1.15	1.02–1.26	0.10									
BaO	3.56	2.90–4.12	0.56									
SiO_2	29.75	29.46–30.02	0.21	29.88	29.60–30.18	0.22	27.80	27.32–28.20	0.35	25.63	25.13–26.02	0.39
UO_3	55.86	55.10–56.29	0.49	56.69	56.01–57.12	0.43	52.49	52.05–53.00	0.40	48.43	48.15–48.90	0.30
H_2O	3.01*			4.73**			1.66**			1.42**		
Total	100.00			100.95			99.48			99.01		

*By deficiency of the total
**Based upon the crystal structure

The empirical formulas calculated on the basis of 17 O atoms per formula unit and respective quantity of H_2O groups based on the deficiency of the total or upon the crystal structure, are as follows: $K_{1.22}Na_{0.30}Ba_{0.23}Ca_{0.21}U_{1.96}Si_{4.96}O_{17}(H_2O)_{2.61}$ for weeksite; $K_{2.06}U_{1.99}Si_{5.00}O_{17}(H_2O)_{2.64}$ for its K-analog; $Rb_{2.03}U_{1.99}Si_{5.01}O_{17}(H_2O)_{1.00}$ for Rb-analog and $Cs_{1.97}U_{1.99}Si_{5.02}O_{17}(H_2O)_{0.93}$ for Cs-analog.

2.5 Powder X-ray analysis

The powder X-ray diffraction data of samples under study (Figure S2) were collected in air on a Rigaku Ultima X-ray diffractometer (Cu*K*α radiation). The samples were prepared from heptane suspensions. The speed of the experiment is 2 º/min. Unit-cell parameters were refined by least-square methods.

2.6 High-temperature powder X-ray diffraction study

The thermal behavior of compounds was studied in air on the same powder X-ray diffractometer (Cu*K*α radiation) with a high-temperature camera Rigaku HTA 1600. The samples were prepared from heptane suspension on a Pt-Rh plate. The temperature step was 20 °C in the range of 25 – 1000 °C. At each temperature, the sample was equilibrated for 15 minutes. Unit-cell parameters at different temperatures were refined by least-squares fits. The main coefficients of the thermal expansion tensor were determined using a linear approximation of temperature dependences by the ThetaToTensor program (Bubnova *et al.*, 2013).

2.7 Infrared spectroscopy

The IR spectra of weeksite and its synthetic analogs were obtained using a standard KBr technique on an ALPHA FTIR spectrometer (Bruker Optics) with a resolution of 4 cm^{-1} and 10 scans.

https://doi.org/10.1180/mgm.2025.10149 Published online by Cambridge University Press

The infrared spectra of mineral, K- and Cs- analogs (Figure S3) were studied in the range 4000 - 400 cm^{-1} and analyzed in comparison with the infrared spectra of synthetic weeksite already described by Plesko *et al*. (1992) and Frost *et al*. (2006). The absorption spectra that we have obtained are highly analogous to those presented earlier (Figure S3).

In the IR spectra bands in the range 870-930 cm^{-1} can be assigned to the antisymmetric stretching mode $\nu_3 (UO_2)^{2+}$ (Čejka, 1999). According to Frost *et al*. (2006), $\nu_1 (SiO_4)^{4-}$, $\nu_2 (SiO_4)^{4-}$, $\nu_4 (SiO_4)^{4-}$ vibrations which describe symmetrical vibrations of stretching and bending of SiO_4 groups are observed in the range 400-900 cm^{-1}. Bands of asymmetric stretching vibrations of SiO_4 groups are observed in the range of 1000-1200 cm^{-1} ($\nu_3 (SiO_4)^{4-}$) (Plesko *et al*., 1992).

Bending vibrations δH_2O are observed in the range 1400-1600 cm^{-1}, HOH bending vibrations lie in the range 1600-1750 cm^{-1}, in the IR spectra described by Čejka (1999) (Figure S3) additional bands of water molecules are also observed in the range 1350-1400 cm^{-1}. Заменено на: The region of O–H- stretching modes oscillations covers the range 3000 - 3500 cm^{-1}. A wide band in this range may be due to the disordered position of water molecules.

2.8 Ion exchange properties of the Rb-analog of weeksite

Ion exchange experiments were performed using a common hydrothermal technique. The crystals of the rubidium compound were placed in a Teflon-lined autoclave containing 5 ml of 2 *M* solution of corresponding alkali chloride; the syntheses were conducted at 180 ºC in 7 days. No exchange was observed at 130 ºC, while above 220 ºC, the crystals dissolve. The successful exchange was observed for solutions of KCl and CsCl but not of NaCl; the reaction products were studied by both EDX and single-crystal X-ray diffraction.

3. Results

3.1 Crystal structure of $A_2[(UO_2)_2(Si_5O_{13})](H_2O)_n$ (A = K, Rb, Cs)

In the crystal structure of $A_2[(UO_2)_2(Si_5O_{13})](H_2O)n$ (*A* = K, Rb, Cs), the uranium atom forms a typical uranyl cation (<U-O_{Ur}> = 1.810, 1.800, 1.793 and 1.814 Å for weeksite, K-, Rb-, Cs-analogs, respectively) coordinated, in the equatorial plane, by five oxygen atoms (<U-O_{eq}> = 2.372, 2.366, 2.391 and 2.378 Å). Three symmetrically independent silicon atoms are tetrahedrally coordinated with <Si-O> = 1.610, 1.612, 1.612 and 1.614 Å, for weeksite, K-, Rb- and Cs-analogs, respectively. In the structure of $A_2[(UO_2)_2(Si_5O_{13})](H_2O)_n$ (*A* = K, Rb, Cs) **(**Figure 2a) UO_7 polyhedra share edges to form chains rather common for uranium minerals, *e.g.* sklodowskite, $Mg[(UO_2)_2(SiO_3OH)_2](H_2O)_6$ (Plášil, 2018), kasolite,

https://doi.org/10.1180/mgm.2025.10149 Published online by Cambridge University Press

$Pb[(UO_2)(SiO_4)](H_2O)_2$ (Fejfarová *et al.*, 2013), and haiweeite, $Ca[(UO_2)_2Si_5O_{12}(OH)_2](H_2O)_6$ (Plášil *et al*, 2013).

The structure of the uranyl silicate framework in all discussed structures is nearly insensitive to the nature of the alkali cation; the differences concern mainly the distribution of the cations and water molecules within the channels. Overall, there are three internal sites, *A*1, *A*2, and *A*3 (Table 3). The respective site occupancies in all studies natural and synthetic compounds were initially refined unrestricted, and fixed at the final stages to provide overall electroneutrality. Note that some of these sites could be refined only isotropically. Unfortunately, the amount of produced crystals was too small for the TGA studies and confirm independently the water content calculated from structural refinements. The positions within the channels are strongly disordered and the amount of water can vary within certain limits.

In the structure of the Rb synthetic analog, the *A*1 site (Fig. 2) is split into two "subsites", Rb1*A* (s.o.f. = 86%) and Rb1*B* (s.o.f. = 14%) at at separation of 2.46(2) Å. The *A*2 site is "tripled"into Rb2*A* (s.o.f. = 56%), Rb2*B* (s.o.f. = 40%), and Rb2*C* (s.o.f. = 2%). The *A*3 is fully and exclusively occupied by water molecules. The highest residual electron density peak is 1.80 e/Å^3 (1.16 Å from U1). Hence, structural study of the Rb compound results in the $Rb_2[(UO_2)_2(Si_5O_{13})](H_2O)_{1.00}$ composition. The coordinates of the *A* sites were used as starting values for the other refinements described below.

Table 3. *A*-sites atomic coordinates and occupancies in studied weeksites.

Sites			**Cs**	**Rb**	**K**	**mineral**
***A*1**			**Cs1*A***	**Rb1*A***	**K1*A*/O1*A***	**K1*A*/O1*A***
	A*1*A	*x*	0.26839(9)	0.26229(13)	0.2433(3)	0.2437(3)
		y	0	0	0	0
		z	0.85578(13)	0.8545(2)	0.8358(5)	0.8379(5)
		Occ.	$Cs_{0.9}$	$Rb_{0.86}$	$K_{0.82}O_{0.18}$	$K_{0.74}O_{0.26}$
	A*1*B		**Cs1*B***	**Rb1*B***	**K1*B*/O1*B***	**K1*B*/O1*B***
		x	0.4218(10)	0.4329(9)	0.4304(5)	0.4306(5)
		y	0	0	0	0
		z	0.8619(11)	0.849(2)	0.8405(10)	0.8407(11)
		Occ.	$Cs_{0.08}$	$Rb_{0.14}$	$K_{0.18}O_{0.82}$	$K_{0.26}O_{0.74}$
	A*1*C		**Cs1*C***	-	-	-
		x	0.220(3)			
		y	0			
		z	0.782(4)			
		Occ.	$Cs_{0.02}$			
***A*2**	***A*2*A***		**Cs2*A***	**Rb2*A***	**K2*A***	**K2*A***
		x	-0.0833(9)	-0.0808(5)	-0.0783(13)	-0.0773(17)
		y	0	0	0	0
		z	0.8114(14)	0.8077(8)	0.766(3)	0.762(4)
		Occ.	$Cs_{0.435}$	$Rb_{0.56}$	$K_{0.44}$	$K_{0.37}$
	A*2*B		**Cs2*B***	**Rb2*B***	**K2*B*/O2*B***	**K2*B*/O2*B***

https://doi.org/10.1180/mgm.2025.10149 Published online by Cambridge University Press

		x	-0.0777(7)	-0.0707(9)	-0.0780(8)	-0.0780(10)
		y	0	0	0	0
		z	0.7833(14)	0.7489(16)	0.818(2)	0.818(2)
		Occ.	$Cs_{0.435}$	$Rb_{0.4}$	$K_{0.15}O_{0.85}$	$K_{0.31}O_{0.69}$
	A*2*C		**Cs2*C***	**Rb2*C***	**K2*C***	**K2*C***
		x	0.071(2)	0.071(3)	0.0759(16)	0.0784(18)
		y	0.069(2)	0.065(3)	0.0562(16)	0.0603(18)
		z	0.531(4)	0.539(4)	0.558(3)	0.562(3)
		Occ.	$Cs_{0.03}$	$Rb_{0.02}$	$K_{0.1}$	$K_{0.12}$
***A*3**	***A*3**		**Cs3/OW**	**OW**	**K3*A*/O3*A***	**K3*A*/O3*A***
		x	-0.2803(10)	-0.2731(8)	-0.2585(6)	-0.2584(6)
		y	0	0	0	0
		z	0.8099(16)	0.8243(13)	0.8448(11)	0.8465(12)
		Occ.	$O_{0.932(8)}Cs_{0.068(8)}$	$O_{1.00}$	$K_{0.82}O_{0.18}$	$K_{0.92}O_{0.08}$

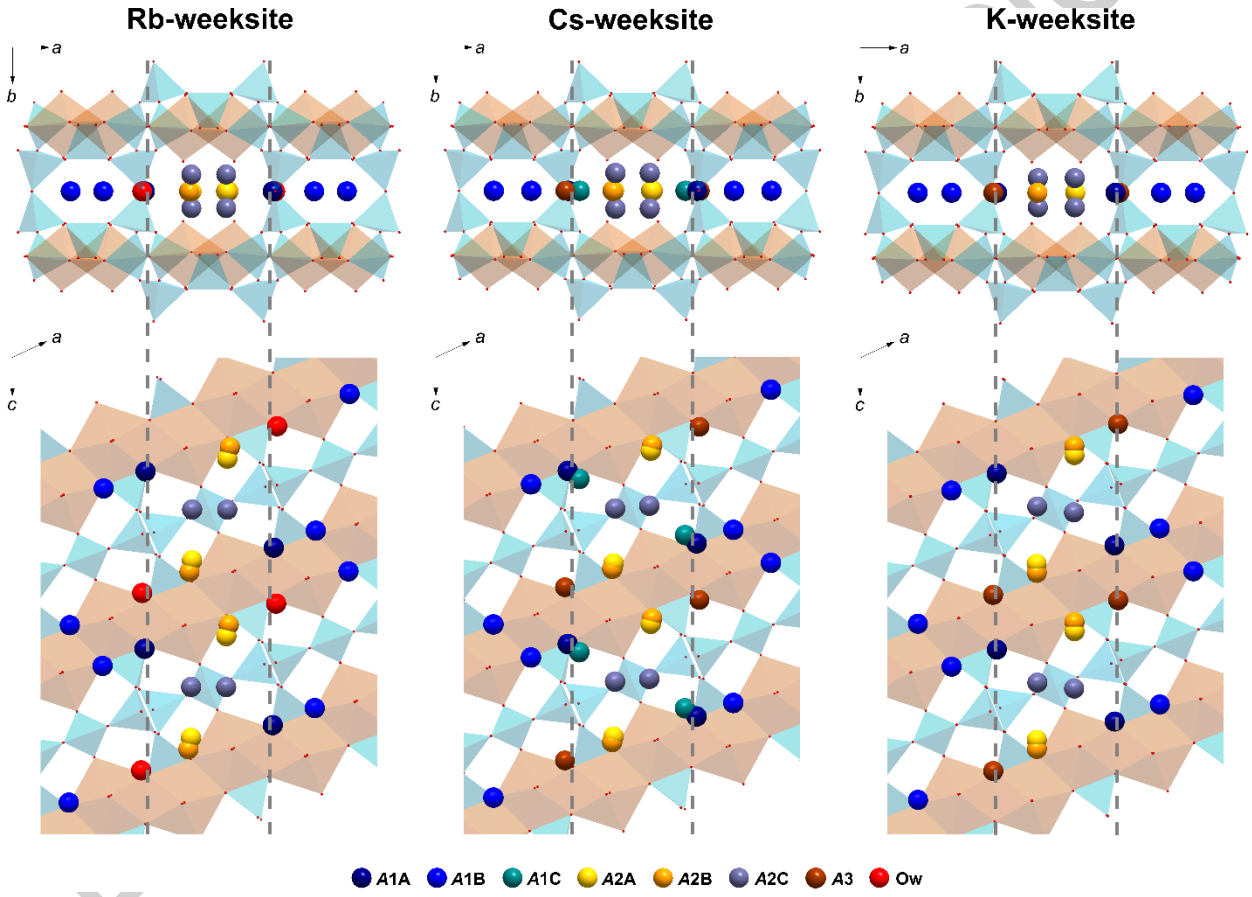

Figure 2. "Intra-channel" sites in the structure of the Rb, Cs, and K weeksite analogs.

In the structure of the Cs compound, contrary to the previous structure, the *A*1 site is "tripled" into Cs1*A* (s.o.f. = 90%), Cs1*B* (s.o.f. = 8%), and Cs1*C* (s.o.f. = 2%). The separations between these vary between 0.78(4) and 2.78(2) Å. The *A*2 is also "tripled" into Cs2*A* (s.o.f. = 43.5%), Cs2*B* (s.o.f. = 43.5%), and Cs2*C* (s.o.f. = 3%). The *A*3 is mixed-occupied by OW (s.o.f. = 93 %) and Cs3 (s.o.f. = 7 %). The highest residual electron density peak of is 2.18 e/Å^3, also very close (1.13 Å) to U1. The calculated formula is therefore

https://doi.org/10.1180/mgm.2025.10149 Published online by Cambridge University Press

$Cs_2[(UO_2)_2(Si_5O_{13})](H_2O)_{0.93}$. A smaller amount of water can be explained by larger volume of Cs^+ compared to Rb^+, and consequently less free space is left for the water molecules .

Due to essentially smaller size of K^+ respective to Rb^+ and Cs^+, there are stronger differences in the fillings of channels. The *A*1 site, akin to the Rb compound, is split into *A*1*A* and *A*1*B* both of which are mixed-occupied by potassium cations and water molecules: *A*1*A* = $(K1)_{0.82}(OW)_{0.18}$, *A*1*B* = $(K1)_{0.18}(OW)_{0.82}$. This agrees to the separations of *A*1*A* - *A*1*B* = 2.645(7) Å and *A*1*A* - *A*1*B* = 2.98(1) Å when considering these as K–OW bonds. The *A*2 is tripled into *A*2*A* (s.o.f. = 44% K^+), *A*2*B* $(K2)_{0.15}(OW2)_{0.85}$, and *A*2*C* (s.o.f. = 10% K^+). Note the mixed potassium – water occupancy of the *A*2*B* while *A*2*A* and *A*2*C* are partially occupied by potassium cations only. The *A*3 is also mixed- occupied by OW3 (s.o.f. = 79 %) and K3 (s.o.f. = 21 %). A residual peak of 2.62 e/Å^3 at 2.46 Å from *A*3 indicates an even more complex disorder in the potassium compound. Yet, attempts to consider the maximum of electron density led to unstable. Hence, the calculated formula for the synthetic K-analog indicated essentially larger amount of water: $K_2[(UO_2)_2(Si_5O_{13})](H_2O)_{2.64}$. Repeat, these data can be considered as tentative and need further verification. Nevertheless, water-content calculations show that the number of molecules pfu drops with increasing alkali radius (for K-, Rb- and Cs-analogs, respectively). This is not surprising, considering that the larger the cation, the less free space is left for the water molecules.

The distribution of K^+ cations and H_2O molecules in the natural mineral is rather similar to that described just above. Again, due to imprecise determination of water content and, in addition, the mixed-cation (Table 1) filling of the respective sites, estimation of water content based on single-crystal refinement is tentative at best. The zeolitic nature of the weeksite structure does not permit unambiguously attributing a given site within the channel to a set of cations and water molecules. All sites were refined as occupied by potassium cations and/or H_2O groups. Given this approximation, the formula can be written as $K_2[(UO_2)_2(Si_5O_{13})](H_2O)_{2.61}$, very close to the value for the synthetic analog.

The bond valence sums, calculated using the parameters from Gagné and Hawthorne, (2015), correlate well to the formal valences of the atoms (Table S5, S8, S11). Bond valence analysis was not performed for weeksite mineral due to the several complex isomorphic substitutions (Table 2). A slight overbonding for the silicon atoms is rather commonly observed among the structures of uranyl silicates (Nazarchuk *et al*., 2022, 2023a,b). Site occupancies were taken into consideration in the calculations.

https://doi.org/10.1180/mgm.2025.10149 Published online by Cambridge University Press

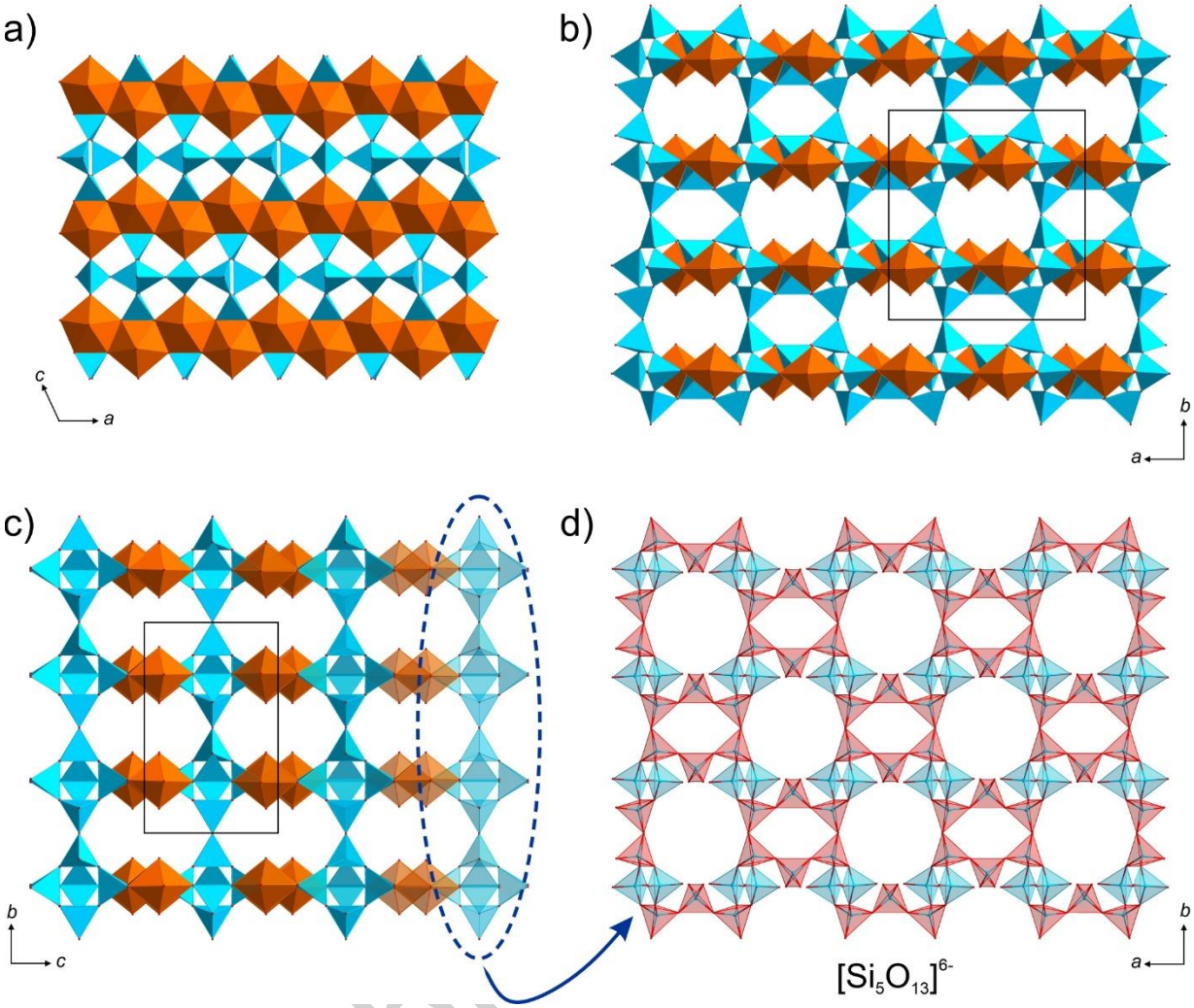

Figure 3. Crystal structure of $A_2[(UO_2)_2(Si_5O_{13})](H_2O)_n$ (A = K, Rb, Cs). Connection of uranium and silicon polyhedra (a). Projection of $A_2[(UO_2)_2(Si_5O_{13})](H_2O)_n$ on the *ab*(b) and *bc*(c) plane. The $^2_\infty[Si_5O_{13}]^{6-}$ layers (d). Uranium polyhedra are shown in brown and silicon in blue. The 6-membered rings $[Si_6O_{18}]^{12-}$ are highlighted in red.

The SiO_4 tetrahedra share vertices to form $[Si_5O_{13}]^{6-}$ layers (Figure 3a) comprised of six-membered $[Si_6O_{18}]^{12-}$ rings linked by $Si2O_4$ tetrahedra (Figure 3d). The chains of uranium polyhedra and $[Si_5O_{13}]^{6-}$ layers form a microporous framework (Figure 3b, c). In the *ab* and *bc* planes, there are relatively wide channels, which host the alkali cations and water molecules. In *ab*, the size of the channels is 6.98×0.98 $Å^2$; in *bc*, their size is 5.00×0.80 and 6.20×6.20 $Å^2$. The increase of the ionic radius of the alkali cation results in expected changes in the unit-cell parameters (Figure 4a). Both *a* and *b* increase while *c* and β decrease; the change in unit-cell volume is nearly linear.

https://doi.org/10.1180/mgm.2025.10149 Published online by Cambridge University Press

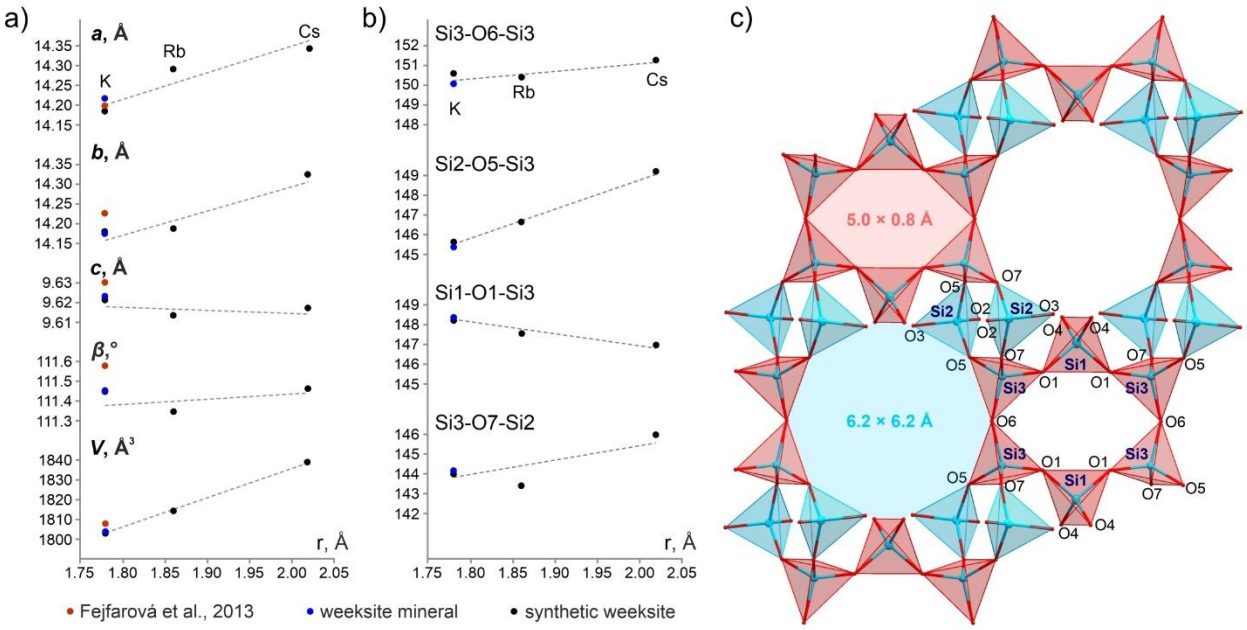

Figure 4. Dependence graph of unit-cell parameters (a) and Si-O-Si angles (b) on the *A* cation radius. The 6-membered rings $[Si_6O_{18}]^{12-}$ and 10-members rings $[(UO_2)_2(Si_8O_{32})]^{28-}$ in the structure of $A_2[(UO_2)_2(Si_5O_{13})](H_2O)_n$. (c). The 6-membered rings $[Si_6O_{18}]^{12-}$ are highlighted in red.

The smaller channels in these structures are formed by $Si1O_4$ and $Si3O_4$ tetrahedra, which share vertices to form six-membered $[Si_6O_{18}]^{12-}$ rings. As a result, flexible Si3-O6-Si3 and Si1-O1-Si3 "hinges" are formed. The Si3-O6-Si3 angle increases linearly while Si1-O1-Si3 decreases when passing from *M* = K to *M* = Cs. (Figure 4b). The larger channels are formed from $Si1O_4$, $Si2O_4$, and $Si3O_4$ tetrahedra (Figure 4c). As a result, four hinges are formed: Si3-O6-Si3, Si3-O7-Si2, Si2-O5-Si3, and Si1-O1-Si3. With increasing alkali radius, the Si3-O7-Si2 and Si2-O5-Si3 increase while Si1-O1-Si3 decreases.

3.3 Thermal expansion of weeksite and $A_2[(UO_2)_2(Si_5O_{13})](H_2O)_n$

3.3.1 Powder X-ray thermal expansion

On the PXRD pattern of weeksite (Figure 5a), the diffraction maxima shift towards higher angles at the initial heating stages (40-200 °C). This can be explained by gradual dehydration. Overall, the anhydrous compound is stable until 860±10 °C, but some additional reflections start to appear above 720±10 °C (Figure 5a) which can be attributed to $K_2U_4O_{13}$ and SiO_2. A similar pattern is observed also for the synthetic potassium compound, but the U-containing decomposition product is $K_2U_7O_{22}$. The difference can be tentatively explained by the presence of other cations in the natural sample. In contrast, the Rb- and Cs-analogs are stable at least until 1000±10 °C (Figure 5b). As the crystal structures of the compounds are topologically identical with the only difference in the nature (size) of the alkali cations, type

https://doi.org/10.1180/mgm.2025.10149 Published online by Cambridge University Press

of their disorder and water content, the difference in thermal behavior can be attributed to the same factors.

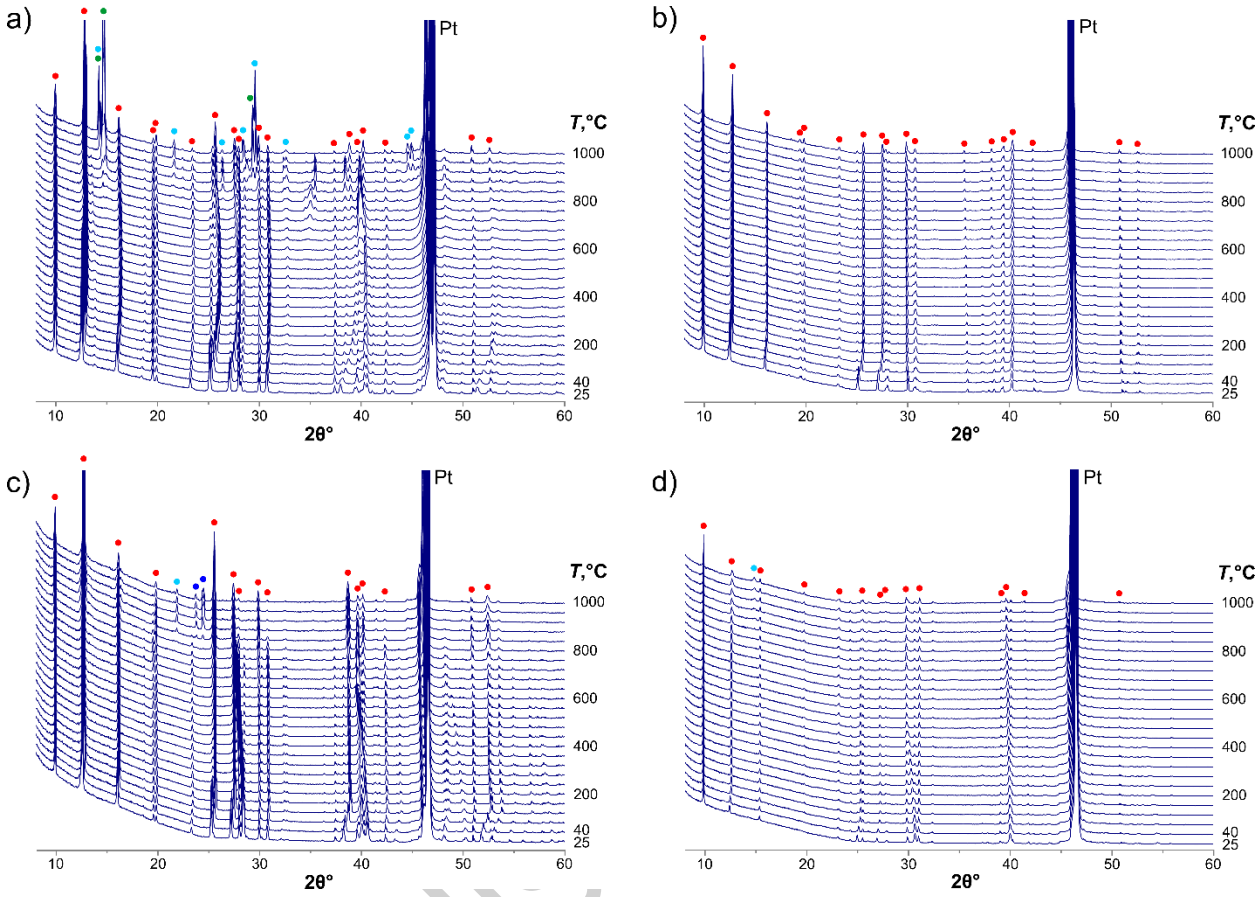

Figure 5. Powder X-ray diffraction pattern of weeksite (a) and Rb - (b), K - (c) and Cs- (d) synthetic analogues. Reflections of $K_2U_4O_{13}$, $K_2U_7O_{22}$, SiO_2, and the initial compound are highlighted in cyan, blue, green, and red, respectively.

The graphs of thermal dependences of unit-cell parameters can be divided into two regions: 20-500 and 500-800 °C for weeksite and 20-150 and 150-800 °C (Figure 6) for the synthetic compounds; overall, the behavior of the mineral and its analogs is different. The slope of the dependence of *b* and *V* for the mineral is flatter, and the dehydration temperature can be estimated as 150-400 °C. Above that, the *b* of the mineral increases sharply in contrast to the synthetic compounds. Similar differences are also observed for *a,* which decreases slightly for the mineral and Rb-analog but drops essentially for the Cs compound.

https://doi.org/10.1180/mgm.2025.10149 Published online by Cambridge University Press

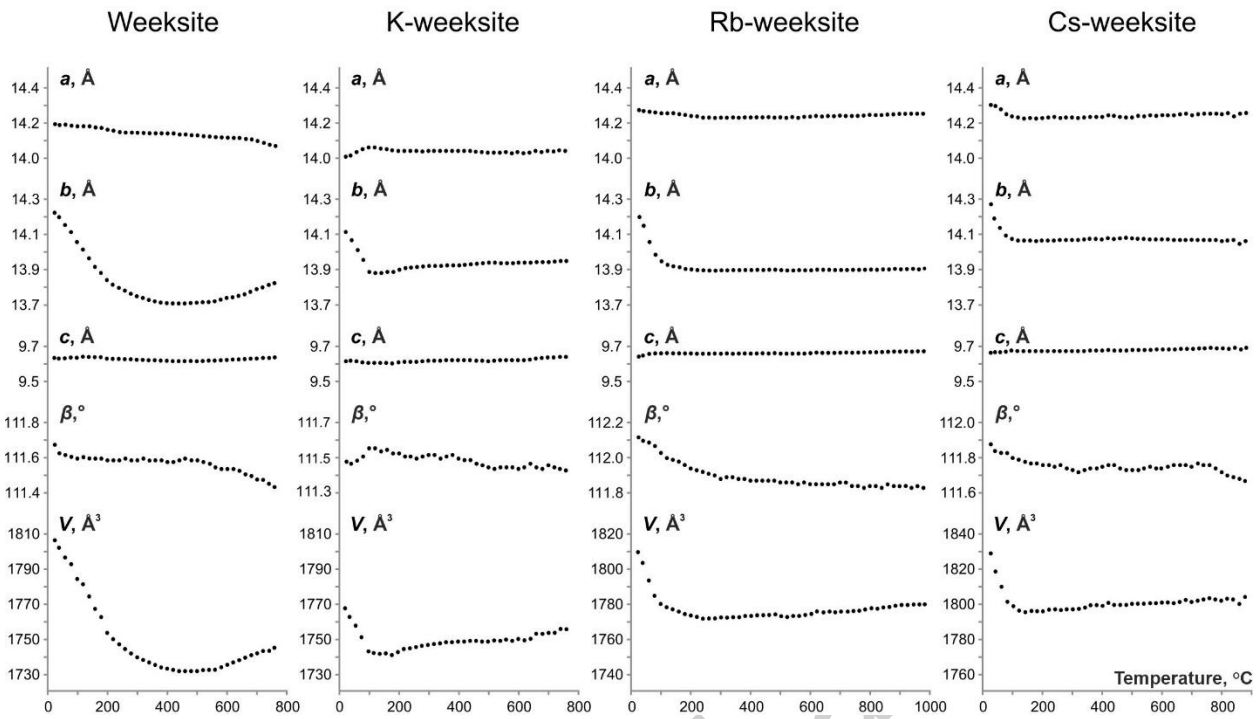

Figure 6. Temperature dependences of the unit-cell parameters and volume for weeksite (a) and K- (b), Rb- (c) and Cs- (d) synthetic analogues.

The thermal expansion of the mineral and its analogs is strongly anisotropic (Figure 7). The structure of the mineral gradually changes the character of its expansion from negative to positive. Between 20 and 500 ºC thermal expansion of weeksite is negative or almost zero in all directions, after 500 ºC, only in the monoclinic plane. The negative thermal expansion decreases from 20 to 500 ºC and after 500 ºC becomes positive in *ab* and *bc* planes.

Between 20 and 150 ºC, the structure of K-, Rb- and Cs-analogues exhibit similar as weeksite negative thermal expansion in *ac* and *ab* planes (Figure 7) due to dehydration processes. Between 120 °C and decomposition points, the behavior of the synthetic analogs is slightly different. The frameworks are sufficiently stable to retain their integrity after dehydration and their expansion can be estimated.

After the dehydration process, the coefficients of thermal expansion for all compounds become similar, but anisotropy is distinct in each case. The thermal expansion of K-weeksite (α_{11} = -1.58, α_{22} = 6.39, α_{33} = 5.19, α_V = 10.0 ×·10^{-6} °C^{-1}) becomes similar to thermal expansion of weeksite (α_{11} = -7.1, α_{22} = 11.5, α_{33} = -0.33, α_V = 4.1 ×·10^{-6} °C^{-1}). The main difference between the thermal behavior of weeksite and its synthetic K-analog is the speed and smoothness of the dehydration process. After 150 ºC the thermal expansion of Rb- (α_{11} = 4.21, α_{22} = 1.10, α_{33} = 1.63, α_V = 6.94 ×·10^{-6} °C^{-1}) and Cs-weeksite (α_{11} = 2.52, α_{22} =

https://doi.org/10.1180/mgm.2025.10149 Published online by Cambridge University Press

0.94, α_{33} = 2.75, α_V = 6.21 ×·10^{-6} °C^{-1}) is very close. In general, the volumetric thermal expansion of all synthesized analogs and weeksite has similar values, the difference can be explained by the nature of the alkali cations.

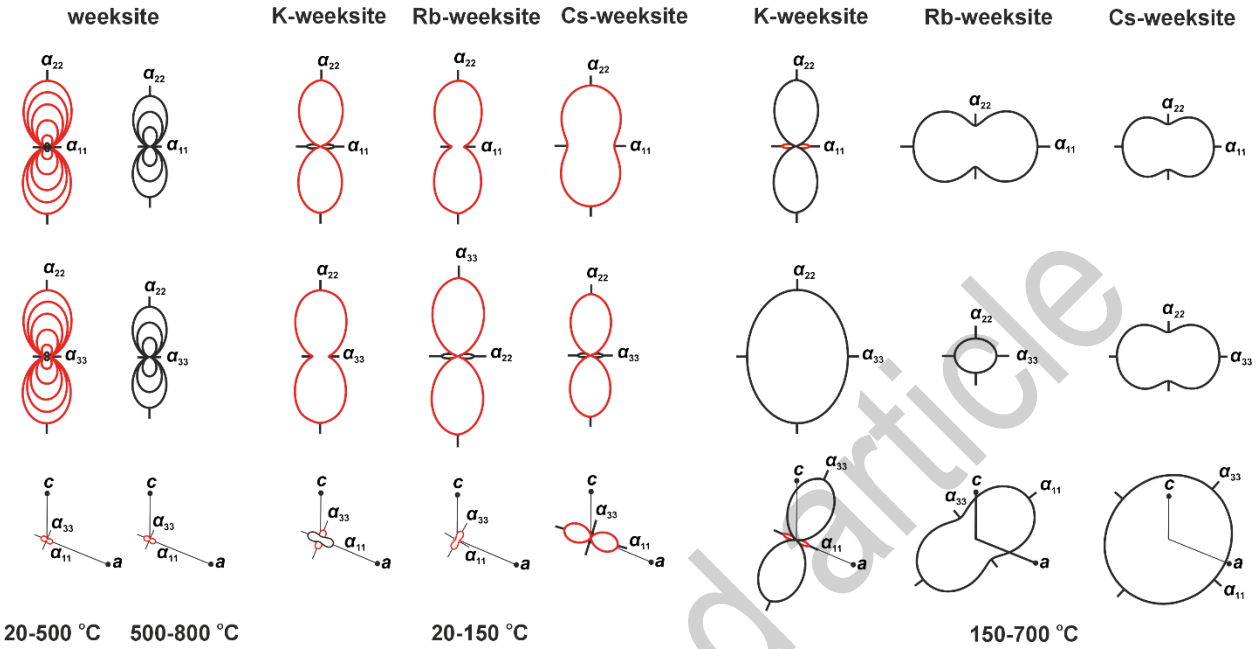

Figure 7. Pole figures of thermal expansion coefficients for weeksite in the temperature ranges 20-500 and 500-800 °C and for K-, Rb-, Cs- analogues in the temperatures 20-800 °C. The red line highlighted negative thermal expansion.

3.3.2 Single crystal X-ray thermal expansion

The single crystal of $Rb_2[(UO_2)_2(Si_5O_{13})](H_2O)$ was found to be stable until 625±25 °C. Below 525 °C, its structure can be refined to acceptable results (see the cif data in the Supplement). Between 525 and 625 °C, the crystal gradually decays, so only cell parameters can be estimated. In the 25 – 525 °C range, the reciprocal space contains a regular set of diffraction maxima. Additional reflections start to appear between 525 and 625 °C, at 625 °C, several nearly spherical arrays are observed, indicating decomposition. At higher temperatures, all maxima disappear.

The thermal evolution of cell parameters is strongly anisotropic (Figure 8a). To confirm the reproducibility of the data, the experiment was conducted twice. Between 25 and 200 °C, the *a*, *b*, β, and *V* decrease, while *c* increases. The largest changes are observed for *b* and can be approximated using a second-term polynomial. Above 200 °C, all parameters increase linearly with temperature. A dramatic change in the thermal behavior of Rb-weeksite can be explained by framework transformations and water loss below 200 °C.

https://doi.org/10.1180/mgm.2025.10149 Published online by Cambridge University Press

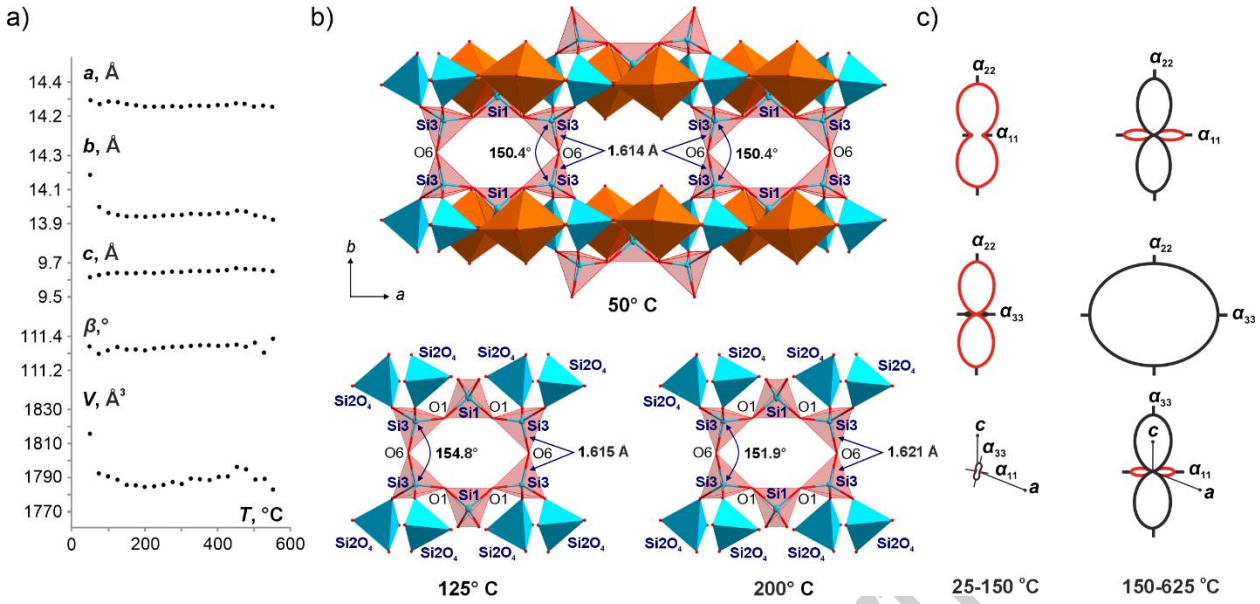

Figure 8. Thermal expansion of the $Rb_2[(UO_2)_2(Si_5O_{13})](H_2O)$ structure. The thermal dependences of the cell parameters (a) and variation of the Si3-O6-Si3 angle (b). Pole figures of thermal expansion coefficients in the temperature ranges 125-525 °C (negative expansion are highlighted in red) (c).

The calculated values for the main components of the thermal expansion tensor also demonstrate its strongly anisotropic character (Figure 8c). Between 25 and 150 ºC, the a_{11} and a_{22} are negative, a_{11}, a_{33} and a_β are nearly constant, while a_{22} increases, becoming positive (Figure 8c). At 150 ºC, the pattern changes and a_{22} and a_{33} coefficients become positive until melting. Between 20 and 150 ºC, the thermal expansion of Rb-analogues exhibits similar trends (α_{11} = -2.8, α_{22} = 11.5, α_{33} = -0.33, α_V = 4.1 $\cdot 10^{-6}$ °C^{-1}) like K-weeksite (α_{11} = -1.58, α_{22} = 6.39, α_{33} = 5.19, α_V = 10.0 $\cdot 10^{-6}$ °C^{-1}).

The anisotropy of thermal expansion of Rb-weeksite can be explained based on some peculiarities of its crystal structure. The framework can be regarded as a series of uranyl silicate layers linked by the $Si3O_4$ tetrahedra (Figure 8b). As a result, a Si3-O6-Si3 “hinge” is formed. Upon temperature increase from 25 to 125 °C, the Si3-O6-Si3 increases from 150.5(5)° to 153.3(8)°, while the Si3-O6 bond shortens from 1.613(3) to 1.602(3) Å. At 200 °C, the pattern is inversed, the Si3-O6-Si3 angle decreases to 151.9(4), while the Si3-O6 separation increases to 1.621(2) Å. Note that the thermal evolution of some bonds remains monotonous at around 200 ºC; the linear dependence is not broken for the <U-O_{ap}>, <U-O_{eq}>, <Si1-O> and <Si2-O> bonds (Figure 6). In contrast, essential changes are observed for the mean bond lengths in the <Si3-O> tetrahedra and for the Si3-O6 bond and Si3-O6-Si3 angle.

https://doi.org/10.1180/mgm.2025.10149 Published online by Cambridge University Press

To sum up, negative thermal expansion persists until the total dehydration at 200 °C, after which a "normal" thermal expansion is observed in all directions.

3.4 Ion-exchange properties of the Rb-weeksite

Under hydrothermal processing in CsCl solutions, the crystals of Rb-weeksite partially or completely exchange Rb^+ by Cs^+, dependent on the processing protocol (Figure 9). This is verified by the results of both EDX and single-crystal studies. Substitution of Rb^+ for Cs^+ essentially enlarges the unit-cell parameters (Table 1). The crystals maintain their integrity and collected diffraction data permit structure refinement to reasonable results in the same *C*2/*m* space group.

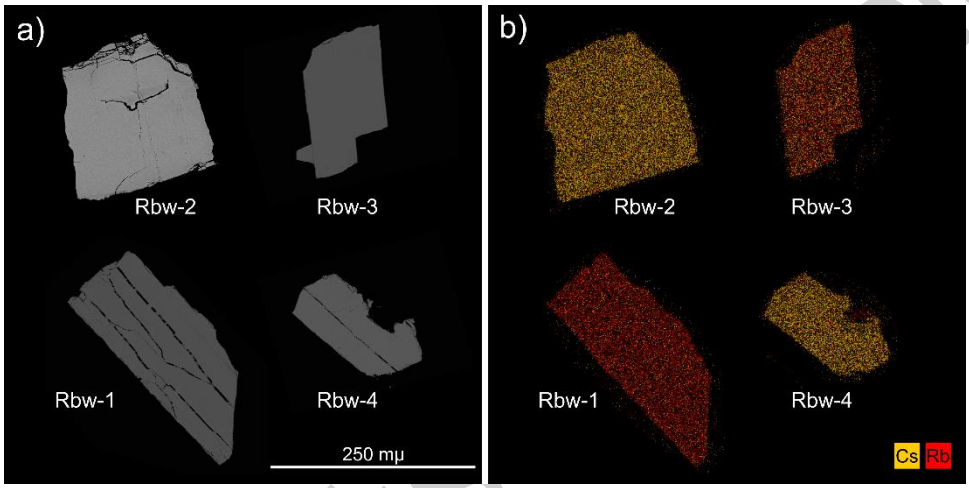

Figure 9. SEM-EDX mapping of $A_2[(UO_2)_2(Si_5O_{13})](H_2O)_n$ (A = Rb, Cs). For each crystal, backscattered electron images and element mapping it presented.

Substitution of Rb^+ by Cs^+ affects the uranyl silicate framework via geometry deformations, which can be estimated by the bonds and angles in the polyhedra at the channel walls. Both channels are symmetric, so for the six-membered rings, it is sufficient to consider Si3- O6, Si3-O1, and Si1-O1 bonds, as well as Si3-O6-Si3 and Si3-O1-Si1 angles (Figure 3c). For the 10-membered rings, we consider Si3-O7, Si2-O7, Si2-O3, U1-O3, and Si3-O6 bonds together with Si3-O7-Si2, Si2-O3-U1, and Si3-O6-Si3 angles. The Si3-O6-Si3 and Si3-O1-Si1 change within ± 0.24°, while Si3-O6, Si3-O1, and Si1-O1, within ±0.01 Å. The rigidity of U and Si polyhedra is reflected also in larger channels: Si3-O7, Si2-O7, Si2-O3, U1-O3, and Si3-O6 vary within ±0.01 Å. The largest changes are observed for the Si3-O7-Si2, Si2-O3-U1, and Si3-O6-Si3 angles. The Si3-O7-Si2 equals 143.3(4)° in the Rb-exchanged compound and 145.9° in the Cs-exchanged sample. Therefore, this angle varies within 2.6 °. The Si2-O3-U1 and Si3-O6-Si vary within 0.73 ° and 1.51 °. These changes lead to shear deformations caused by the changing size of the alkali cations. It is important to note

https://doi.org/10.1180/mgm.2025.10149 Published online by Cambridge University Press

that no substitution was observed under the same conditions by Na^+, K^+ or Ag^+ despite that both K- and Na-based synthetic weeksite analogs have been reported. Therefore, it is likely that under mild hydrothermal conditions, which are more or less close to those in SNF storage sites, *in situ* formed weeksite can behave as a matrix for selective immobilization of radioactive Cs^+ cations in the presence of ubiquitous Na^+ and K^+, despite the closeness of ionic radii ratios: $r(K^+)/r(Rb^+)$ or $r(Rb^+)/r(Cs^+)$. Therefore, it is highly interesting to study the ion exchange properties of Na- and K-based synthetic analogs of weeksite; some of these are currently underway.

Concluding remarks

The mineral weeksite is stable in a wide range of conditions. In nature, it is formed as a product of the relatively mild hydrothermal transformation of the parental rocks. In laboratory conditions, its analogs can be produced via both hydrothermal and solid-state routes. Our results demonstrate that the synthetic analogs of weeksite can be also produced from melts using activated silica tubes and U_3O_8 as the uranium source.

The crystal structure of the mineral is based on a microporous uranyl silicate framework wherein the channels contain (disordered) alkali cation and water sites. Thou the degree of hydration may vary depending on the external conditions, *e.g.* relative humidity even at room temperature, the silicate framework remains stable upon thermal treatment and ion exchange processes. The exchange capacity is to a certain extent similar to that of zeolites, yet the processes are selective. For instance, Rb^+ can be easily substituted by K^+ and Cs^+, yet no substitution was observed under the same conditions by Na^+ or Ag^+ even though both K- and Na-based synthetic weeksite analogs have been reported. The mineral's ability to exchange cations indicates that it can participate in the radionuclide migration.

We were able to refine the structures of both the weeksite itself and its synthetic K-, Rb-, and Cs-analogs. Unfortunately, the distribution of the alkali cations and water molecules in the channels, particularly in the case of potassium, remains obscure. The quality of the crystals, as well as their dehydration under an X-ray beam, essentially affect the data quality. As yet, the synthetic protocols do not permit production of essential amounts of pure compounds for thermal analyses. The shape of crystals is also dependent on the alkali cations. Those of the Cs-analog are mostly platelets. New and helpful data can also be obtained using polythermal single-crystal diffraction of the Cs- and K-analogs; attempts to prepare crystals of the required size and quality have yet not been successful.

Acknowledgments

https://doi.org/10.1180/mgm.2025.10149 Published online by Cambridge University Press

Technical support by the X-Ray Diffraction (project # 118201839) and Geomodel Resource Centers of Saint-Petersburg State University is gratefully acknowledged. This work was financially supported by the Russian Science Foundation through the grant 23-27-00153.

Reference

Babo J.-M. and Albrecht-Schmitt T.E. (2013) High temperature synthesis of two open- framework uranyl silicates with ten ring channels: $Cs_2(UO_2)_2Si_8O_{19}$ and $Rb_2(UO_2)_2Si_5O_{13}$. *Journal of Solid State Chemistry*, **197**, 186-190.

Baturin S.V. and Sidorenko G.A. (1985) Crystal structure of weeksite $(K_{0.62}Na_{0.38})_2(UO_2)_2[Si_5O_{13}]\times 3H_2O$. *Soviet Physics Doklady*, **30**, 435–437.

Bubnova R.S., Firsova V.A. and Filatov S.K. (2013) Software for determining the thermal expansion tensor and the graphic representation of its characteristic surface (theta to tensor-TTT). *Glass Physics and Chemistry*, **39**, 125-128.

Burns P.C., Ewing R.C. and Miller M.L. (1997) Incorporation mechanisms of actinide elements into the structures of U^{6+} phases formed during the oxidation of spent nuclear fuel. *Journal of Nuclear Materials*, **245**, 1-9.

Burns P.C., Olson R.A., Finch R.J. and Hanchar J.M. (2000) $KNa_3(UO_2)_2(Si_4O_{10})_2(H_2O)_4$, a new compound formed during vapor hydration of an actinide-bearing borosilicate waste glass. *Journal of Nuclear Materials*, **278**, 290-300.

Chen F., Burns P.C. and Ewing R.C. (2000) Near-field behaviour of ^{99}Tc during the oxidative alteration of spent nuclear fuel. *Journal of Nuclear Materials*, **278**, 225-232.

Chernikov A.A., Sidorenko G.A. and Valueva A.A. (1977) New data on uranyl minerals of the ursilite-weeksite group. *Zapiski Vserossiyskogo Mineralogicheskogo Obshchestva*, **106**, 553-564 (in Russian).

Chernikov A.A., Sidorenko G.A. and Valuyeva A.A. (1978) New data on uranyl minerals in the ursilite-weeksite group, *International Geology Review*, **20**, 1347-1356.

Chernorukov N.G., Knyazev A.V., and Sazonov A.A. (2007) Synthesis and study of compounds $A^I_2(UO_2)_2Si_5O_{13}\ 3H_2O$ (A^I = Na, K). *Radiokhimiya*, **49**, 114-115.

Čejka, J. (1999) Infrared Spectroscopy and Thermal Analysis of the Uranyl Minerals". Uranium: Mineralogy, Geochemistry, and the Environment, edited by Peter C. Burns and Robert J. Finch, Berlin, Boston: De Gruyter, 521-622.

Cook H.D., Rettger C.J. and Sewalk W.J. (1964) Investigations of burnup determinations on highly irradiated fuels by mass spectrometric methods. *Bettis technical review WAPD-BT-30*, 31-39.

https://doi.org/10.1180/mgm.2025.10149 Published online by Cambridge University Press

Downs R.T. (2000) Analysis of harmonic displacement factors. In: High-temperature and high-pressure crystal chemistry (Eds. R. M. Hazen, R. T. Downs). *Reviews in Mineralogy and Geochemistry*, **41**, 61- 87.

Fejfarová K., Plášil J., Yang H., Čejka J., Dušek M., Downs R.T., Barkley M.C. and Škoda R. (2012) Revision of the crystal structure and chemical formula of weeksite, $K_2(UO_2)_2(Si_5O_{13})\cdot 4H_2O$, *American Mineralogist*, **97**, 750-754.

Fejfarová, K., Dušek, M., Plášil, J., Čejka, J., Sejkora, J. and Škoda, R. (2013) Reinvestigation of the crystal structure of kasolite, $Pb[(UO_2)(SiO_4)](H_2O)$, an important alteration product of uraninite, UO_{2+x}. *Journal of Nuclear Materials*, **434(1)**, 461-467.

Finch R.J., Buck E.C., Finn P.A. and Bates J.K. (1999) Oxidative corrosion of spent UO_2 fuel in vapor and dripping groundwater at 90°C. *Materials Research Society Symposium Proceedings*, **556**, 431-438.

Frost R.L., Čejka J., Weier M.L., Martens W. and Kloprogge J.T. (2006) A Raman and infrared spectroscopic study of the uranyl silicates - weeksite, soddyite and haiweeite. *Spectrochimica Acta*, *A***64**, 308-315.

Gagné & Hawthorne (2015) Comprehensive derivation of bond-valence parameters for ion pairs involving oxygen. *Acta Crystallographica*, *B***71**, 562-578.

Jackson J.M. and Burns P.C. (2000) A reevaluation of the structure of weeksite, a uranyl silicate framework mineral. *Canadian Mineralogist*, **39**, 187-195.

Nazarchuk E.V., Siidra O.I., Charkin D.O. and Tagirova Y.G. (2022) U(VI) coordination modes in complex uranium silicates: $Cs[(UO_6)_2(UO_2)_9(Si_2O_7)F]$ and $Rb_2[(PtO_4)(UO_2)_5(Si_2O_7)]$. *Chemistry*, **4**, 1515-1523.

Nazarchuk E.V., Siidra O.I., Charkin D.O. and Tagirova Y.G. (2023a) Framework uranyl silicates: crystal chemistry and a new route for the synthesis. *Materials*, **16**, 4153.

Nazarchuk E.V., Siidra O.I., Charkin D.O. and Tagirova Y.G. (2023b) Uranyl silicate nanotubules in $Rb_2[(UO_2)_2O(Si_3O_8)]$: synthesis and crystal structure. *Zeitschrift für Kristallographie - Crystalline Materials*, **238**, 349-354.

Oji L.N., Martin K.B., Stallings M.E. and Duff M.C. (2006) Conditions conducive to forming crystalline uranyl silicates in high caustic nuclear waste evaporators. *Nuclear Technology*, **154**, 237-246.

Outerbridge W.F., Staatz M.H., Meyrowitz R. and Pommer A.M. (1960) Weeksite, a new uranium silicate from the Thomas Range, Juab County, Utah. *American Mineralogist*, **45**, 39-52.

https://doi.org/10.1180/mgm.2025.10149 Published online by Cambridge University Press

Petříček, V., Dušek, M. and Plášil, J. (2016) Crystallographic computing system Jana2006: solution and refinement of twinned structures. *Zeitschrift für Kristallographie - Crystalline Materials,* **231**(10), 583-599.

Petříček, V., Dušek, M., Plášil, J. and Palatinus, L. (2023) Jana2020 - a new version of the crystallographic computing system Jana. *Zeitschrift für Kristallographie - Crystalline Materials,* **229**, 345–352.

Plášil, J. (2018) Mineralogy, Crystallography and Structural Complexity of Natural Uranyl Silicates. *Minerals*, **8(12)**, 551.

Plášil, J., Fejfarová, K., Čejka, J., Dušek, M., Škoda, R., Sejkora, J. (2013) Revision of the crystal structure and chemical formula of haiweeite, $Ca(UO_2)_2(Si_5O_{12})(OH)_2{\cdot}6H_2O$. *American Mineralogist*, **98(4)**, 718-723.

Plesko E.P., Scheetz B.F. and White W.B. (1992) Infrared vibrational characterization and synthesis of a family of hydrous alkali uranyl silicates and hydrous uranyl silicate minerals. *American Mineralogist,* **77**, 431-437.

Sheldrick G.M. (2015) Crystal structure refinement with SHELXL. *Acta Crystallographica, C***71**, 3-8.

Wronkiewicz D.J., Bates J.K., Wolf S.F. and Buck E.C. (1996) Ten-year results from unsaturated drip tests with UO_2 at 90°C: implications for the corrosion of spent nuclear fuel. *Journal of Nuclear Materials*, **238**, 78-9.

Yanzhong L. and Jianzhu C. (2002) Fission product release and its environment impact for normal reactor operations and for relevant accidents. *Nuclear Engineering and Design*, **218**, 81- 90.

Yeremenko G.K., Il'menov Ye.S. and Azimi N.A. (1977) Find of weeksite-group minerals in Afghanistan. *Doklady Akademii Nauk SSSR Earth Science Sections*, **237**, 226-228.

Zhu L., Hou X. and Qiao J. (2021) Determination of ^{135}Cs concentration and $^{135}Cs/^{137}Cs$ ratio in waste samples from nuclear decommissioning by chemical separation and ICP-MS/MS. *Talanta*, **221**, 123637.

https://doi.org/10.1180/mgm.2025.10149 Published online by Cambridge University Press